Supporting Information

Dual-Modulation of Electronic Structure and Active Sites of PtCu Nanodendrites by Surface Nitridation to Achieve Efficient Methanol Electrooxidation and Oxygen Reduction Reaction

TianShan Song,[a] Hui Xue,*[,a] Niankun Guo,[a] Jing Sun,[a] Ling Qin,[a] Lei Guo,[a] Keke Huang,[b] Feng He,[c] and Qin Wang*[,a]

[a] College of Chemistry and Chemical Engineering, Inner Mongolia University

Hohhot 010021, P. R. China

[b] State Key Laboratory of Inorganic Synthesis and Preparative Chemistry

Jilin University, Changchun 130022, P. R. China

[c] Institute of Chemistry, Chinese Academy of Sciences, Beijing 100190, P. R. China

University of Chinese Academy of Sciences, Beijing 100190, P. R. China

*Corresponding author: Prof. Dr. Q. Wang, qinwang@imu.edu.cn

Experimental

Chemicals

Chloroplatinic acid hexahydrate ($H_2PtCl_6 \cdot 6H_2O$), N, N-dimethylformamide (DMF), pyridine, ethanol, methanol, perchloric acid, and L-ascorbic acid (AA) were all purchased from Tianjin Fengchuan chemical reagent technology Ltd. Copper (II) chloride dihydrate ($CuCl_2 \cdot 2H_2O$) was obtained from Sinopharm Chemical Reagent Co Ltd. Hexadecyltrimethylammonium chloride (CTAC) was purchased from Shanghai Runjie chemical reagent technology Ltd. A carbon supported Pt catalyst (Pt/C-JM, 20 wt. %). All reagents were analytical grade and used without further treatments. Deionized water was used for all experiments.

Synthesis of PtCu NDs

Typically, 100 mg of CTAC, 100 mg of AA, 2 mL of $H_2PtCl_6 \cdot 6H_2O$ (20 mmol), 70 μl of $CuCl_2 \cdot 2H_2O$ (0.6 mol), 50 μl of DMF, and 4.95 mL of deionized water were mixed and stirred for 30 min at ambient temperature. Then, a homogeneous solution was obtained and transferred into a 20 mL of autoclave and heated at 160 °C for 10 h. After cooled down to room temperature, the as-obtained PtCu NCs was obtained by centrifugation and washed with deionized water and ethanol for several times. Then, the product was dried in a vacuum oven at 70 °C for 8 h.

Synthesis of PtCu-N NDs

In a typical synthesis, the PtCu NCs was added into pyridine and refluxed at 70 °C for 10 h. After that, PtCu-N NDs was obtained by centrifugation and washed with deionized water and ethanol for several times. Then, the product was dried in a vacuum oven at 70 °C for 8 h.

Characterization

The crystal structure and crystallinity of the catalyst were performed on a PuXi XD3 diffractometer (Cu Kα, λ=0.15406 nm). The valence states and compositions were measured on a PHI-5000 X-ray photoelectron spectroscopy (XPS) using Al Kα radiation. Transmission electron microscopy (TEM) and elemental mapping results were obtained by a JEOL-2100F apparatus at 200 kV. High-resolution TEM (HRTEM) image was carried out on a FEI Tecnai G2F30 apparatus at 300 kV.

Electrochemical measurements

Electrochemical measurement was carried out by a three electrode system. The graphite rod, Ag/AgCl (3M), and glassy carbon (0.0707 cm^2, 3.0 mm in diameter) were used as counter electrode, reference electrode, and working electrode, respectively. 5 mg of catalyst was added into a 1 mL of mixture of Nafion (5%), deionized water, and ethanol solution to form an ink (V_{Nafion}: V_{water}: $V_{ethanol}$ =1: 10: 30). Then 2 μL of the ink was smeared onto the working electrode. Methanol oxidation reaction (MOR) measurement：Voltammetric measurements were performed on a CHI 760E electrochemical workstation with a three-electrode system. The glassy carbon, Ag/AgCl (3M), and graphite rod were used as working electrode, reference electrode, and counter electrode, respectively. Before each experiment, the electrode potential was cycled from -0.2 V to

1.0 V vs. Ag/AgCl at a scan rate of 200 $mV \cdot s^{-1}$ until a stable voltammogram was obtained in N_2-saturated 0.5 M H_2SO_4 solution. The electrochemically active surface area (ECSA) of the catalyst was determined based on calculating the hydrogen under the potential desorption (Hupd) area of the CVs. The ECSA of the catalyst can be calculated by the following equation:

$$ECSA = \frac{Q}{C \times m} \quad (2)$$

where Q is the charge passed during the hydrogen adsorption/desorption from the electrode surface after the double layer correction, C (210 $mC \cdot cm^{-2}$) is the charge needed to oxidize a monolayer of H_2 on the Pt catalyst, and m represents the amount of Pt on the electrode surface (mg), respectively. After potential cycling, CVs for the MOR were obtained from -0.2 V to 1.0 V at a scan rate of 100 $mV \cdot s^{-1}$. The N_2-saturated 0.5 M H_2SO_4 and 1.0 M methanol solutions were used as the testing solution. Chronoamperometry measurements were performed at a fixed potential for 4000 s in a solution containing 0.5 M H_2SO_4+1.0 M CH_3OH. For each catalyst, the current was normalized to the loading of noble metals (Pt) to obtain mass activity. All experiments were conducted at room temperature.

Oxygen reduction reaction (ORR) measurement: ORR measurements were performed on a CHI 760E electrochemical workstation with a three-electrode system. The glassy carbon, Ag/AgCl (3 M), and graphite rod were used as working electrode, reference electrode, and counter electrode, respectively. Before each experiment, the electrode potential was cycled from 0.9 V to -0.2 V vs. Ag/AgCl at a scan rate of 200 $mV \cdot s^{-1}$ until a stable voltammogram was obtained in N_2-saturated 0.1 M $HClO_4$ solution. The ORR performance was investigated by cyclic voltammetry (CV) in N_2-saturated 0.1 M $HClO_4$ at a scan rate of 100 $mV \cdot s^{-1}$ at room temperature. Linear sweep

voltammetry (LSV) was performed in the potential range from 0.9 to -0.2 V vs. Ag/AgCl at various rotation rates (400-2000 rpm) in 0.1 M $HClO_4$ under constant O_2 gas flow, with a sweeping rate of 10 $mV \cdot s^{-1}$. The potentials can be converted into reversible hydrogen electrode (RHE) according to the following equation:

$$E_{RHE} = E_{appl} + E_{Ag/AgCl} + 0.059\ pH \quad (3)$$

The corresponding Koutecky–Levich plots were analyzed at different potentials. The slopes of the linear fitting lines were used to calculate the number of transferred electrons (n) by the following Koutecky–Levich equation:

$$\frac{1}{j} = \frac{1}{j_k} + \frac{1}{j_d} = \frac{j}{j_k} + \frac{1}{B\varpi^{1/2}} \quad (4)$$

$$B = 0.62nFC_0D_0^{2/3}v^{-1/6} \quad (5)$$

where j is the measured current, j_k is the kinetic current, j_d is the diffusion-limiting current, w is the rotating speed, n is the number of transferred electrons, F is the Faraday constant (96485 C mol^{-1}), C_0 is the oxygen solubility (1.2×10^{-3} $mol \cdot L^{-1}$), D_0 is the oxygen diffusivity (1.93×10^{-5} $cm^2 \cdot s^{-1}$), and v is the kinetic viscosity of the electrolyte (0.01 $cm^2 \cdot s^{-1}$). The accelerated stability test (ADT) was carried out in 0.1 M $HClO_4$ from 0.9 V and -0.2 V at a scan rate of 200 $mV \cdot s^{-1}$ for 10000 cycles.

CO-stripping voltammograms were obtained by immersing the electrode in a CO-saturated 0.1 M $HClO_4$ solution under a CO blanket for 30 min at a scan rate of 50 $mV \cdot s^{-1}$, running up from 0.9 to -0.2 V at 50 $mV \cdot s^{-1}$. It can be used to calculate the electrochemically active surface area (ECSA) of the catalyst. For each catalyst, the current was normalized to the area amount of Pt to obtain

specific activity, and all of the potentials recorded in this part are given with respect to a reversible hydrogen electrode (RHE) by related calculations. All experiments were conducted at room temperature.

The electron transfer number (n) and the peroxide yield (% H_2O_2) could be calculated as follows:

$$n = \frac{4I_D}{(I_D N + I_R/N)} \quad (6)$$

$$\%H_2O_2 = \frac{200I_R}{(I_R N + I_R)} \quad (7)$$

where I_D is the disk current; I_R is the ring current; and N = 0.4286 is the current collection efficiency of the Pt ring.

Computational Details

Method. The density functional theory (DFT) calculations were performed by using the Vienna ab-initio simulation package (VASP).[1] The projector augmented wave (PAW) method [2] was used and the generalized gradient approximation (GGA) of Perdew-Burke-Ernzerhof (PBE) approach was adopted.[3] An energy cutoff of 400 eV and the 3×3×1 Monkhorst–Pack sampling was applied.[4] Geometries were optimized until the energy was converged to 10^{-6} eV/atom and the force was converged to 10^{-2} eV/Å, respectively. To consider the van der Waals (vdW) interaction, the DFT-D3 force-field approach was employed.

According to the method developed by Rossmeisl and Nørskov et al,[5] the free energy change from initial states to final states of the reaction is calculated as follows:

$$\Delta G = \Delta E + \Delta ZEP - T\Delta S + \Delta G_U + \Delta G_{pH} + \Delta G_{field}$$

where ΔE is the total energy change obtained from DFT calculations, ΔZPE is the change in zero-point energy, T is room temperature (298.15 K), and the ΔS is the change in entropy. The harmonic vibrational frequency calculations were performed to obtain the Zero Point Energy (ZPE) and entropy corrections. ΔG=-eU, where U is the electrode potential with respect to standard hydrogen electrode, and e is the transferred charge. $\Delta G_{pH}=k_B T\ln10*pH$, where k_B is the Boltzmann constant, and pH=0 for acid medium.[6,7] ΔG_{field} is the free energy correction due to the electrochemical double layer and is neglected as in previous studies.[6, 7]

Model. The (111) surface is observed by XRD in experiment and is obtained by cutting PtCu along [111] direction. A four layers and 3×4 supercell of surface was chosen. The Cu-N bond is observed by XPS in experiment. The PtCu (111) surface with Cu-N is constructed on the outmost surface by adding onean N atom. In all structural optimization calculations, the bottom two layers are fixed, while the positions of the other atomic layers were allowed to relax. To avoid periodic interactions, a vacuum layer as large as 15 Å was used along the z direction normal to the surface.

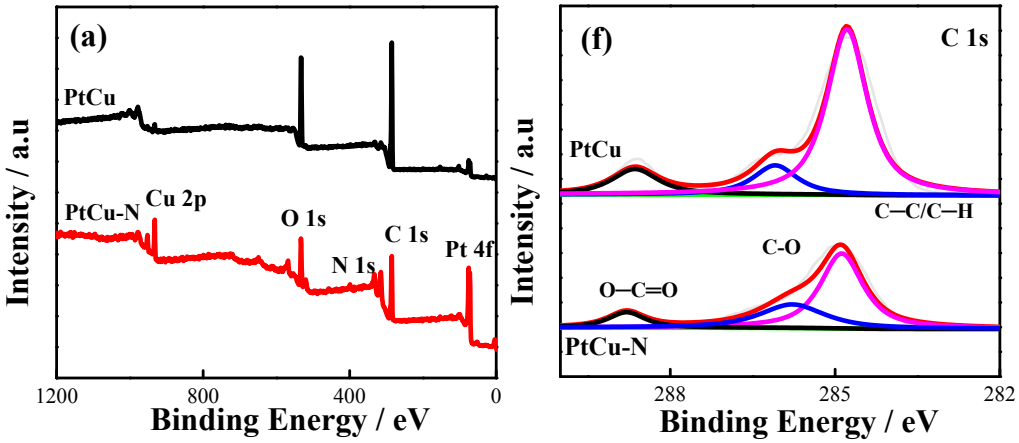

Fig. S1 XPS spectra of the PtCu and PtCu-N catalysts: (a) survey spectrum and (b) C 1s.

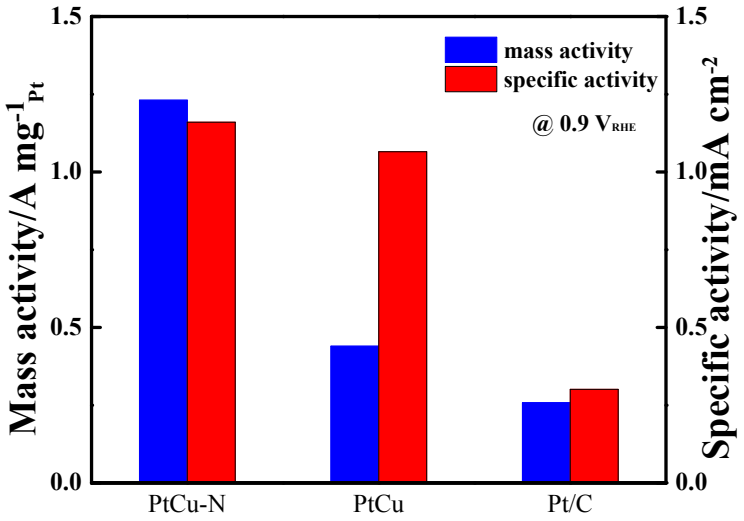

Fig. S2 Specific activity and mass activity of PtCu-N NDs at 0.9 V_{RHE}.

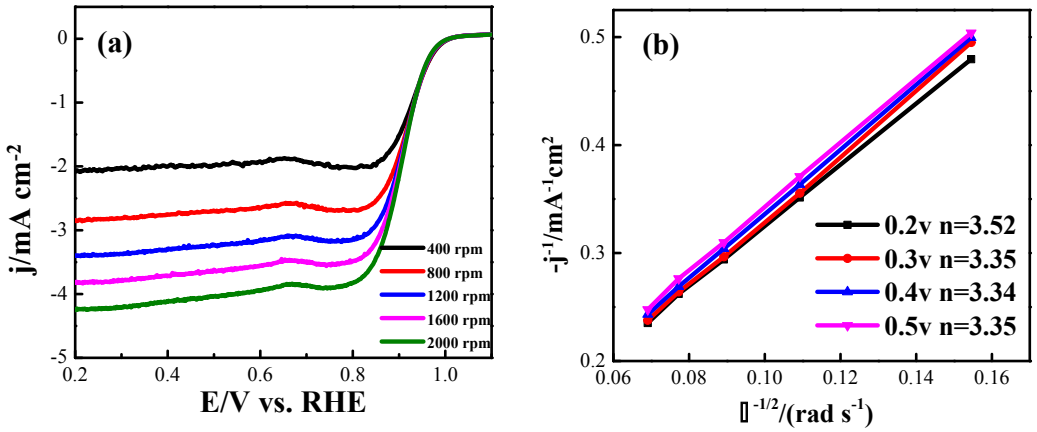

Fig. S3 (a)ORR polarization curves of PtCu-N NDs at different rotation rates, (b) the number of transferred electrons at different potentials.

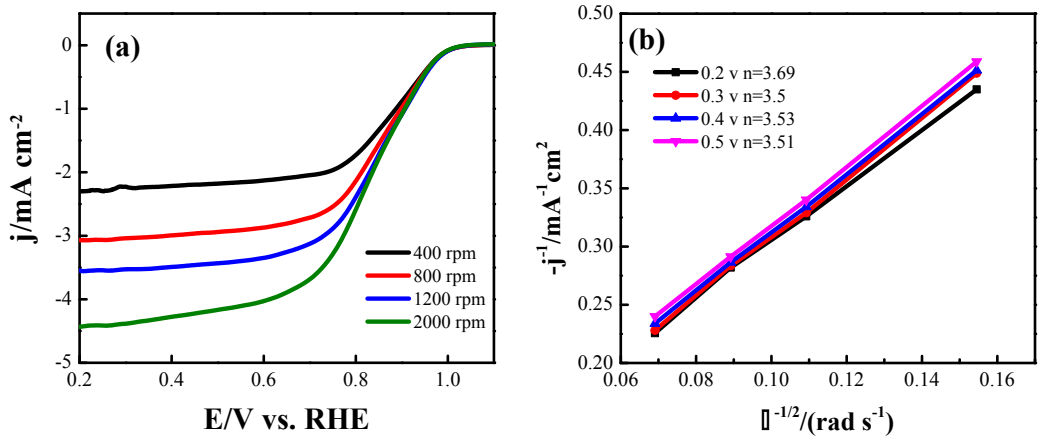

Fig. S4 (a)ORR polarization curves of PtCu NDs at different rotation rates, (b) the number of transferred electrons at different potentials.

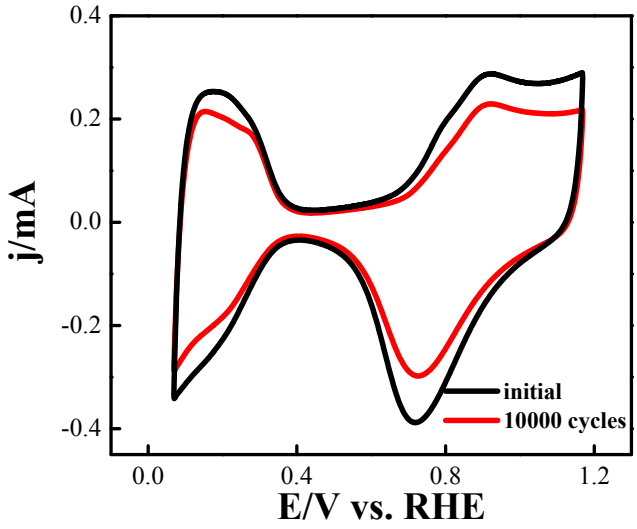

Fig. S5 ORR property of the commercial PtCu-N NDs catalysts. CVs of these catalysts before and after the stability test of 10000 potential scans.

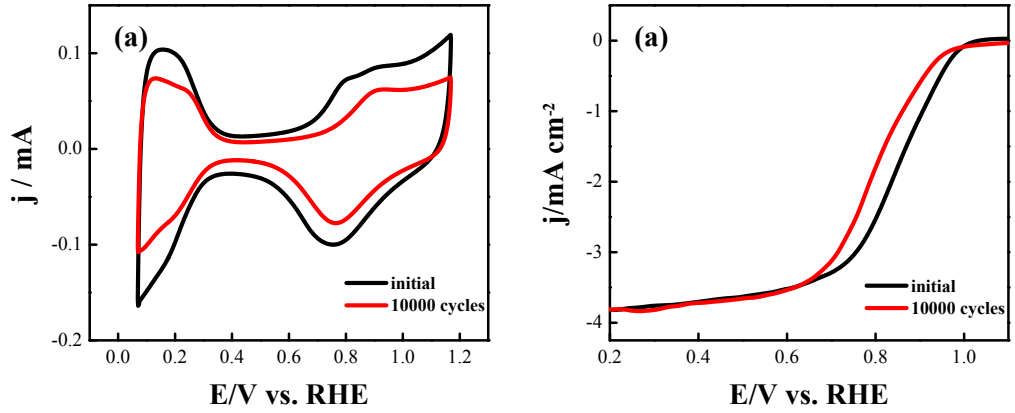

Fig. S6 ORR property of the PtCu NDs catalysts. (a) CVs of these catalysts before and after the stability test of 10000 potential scans, (b) ORR polarization curves of these catalysts before and after the stability test of 10000 potential scans.

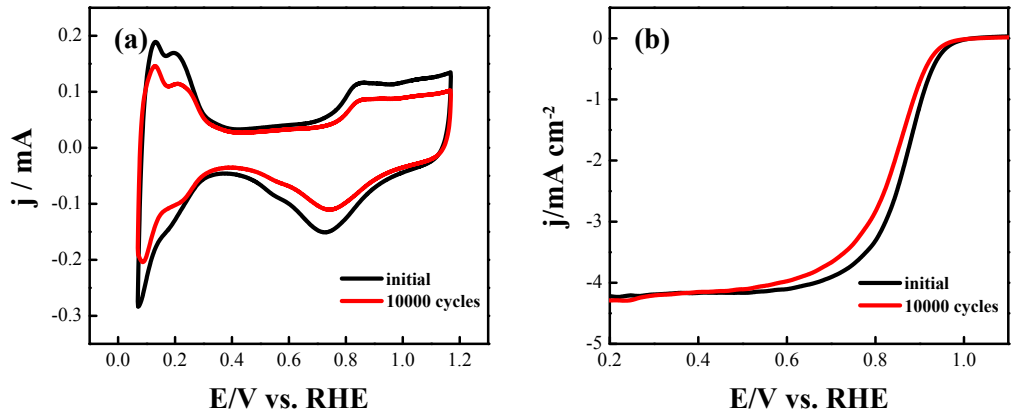

Fig. S7 ORR property of the commercial Pt/C catalysts. (a) CVs of these catalysts before and after the stability test of 10000 potential scans, (b) ORR polarization curves of these catalysts before and after the stability test of 10000 potential scans.

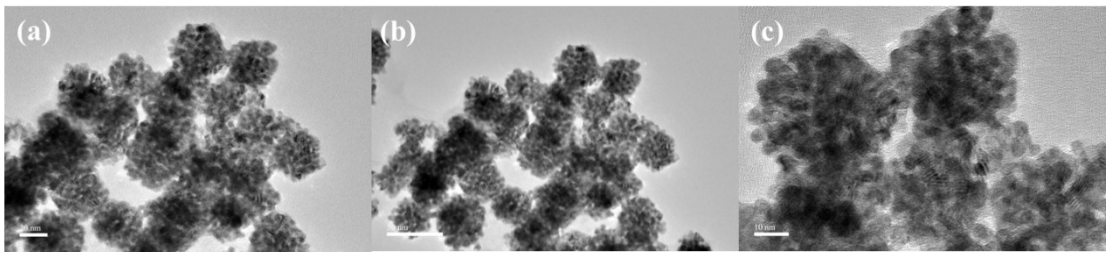

Fig. S8 (a-c) Low and high magnification TEM image and after the stability test of 10000 potential scans.

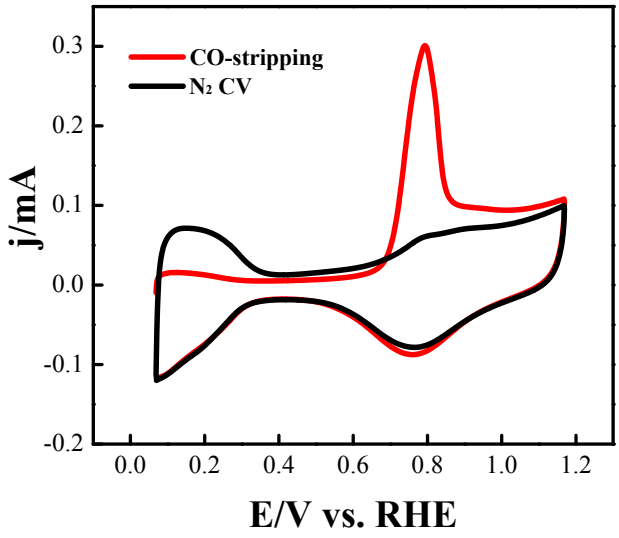

Fig. S9 CO-stripping voltammograms over PtCu NDs in a CO-saturated 0.1 M $HClO_4$ solution at a scan rate of 50 $mV \cdot s^{-1}$.

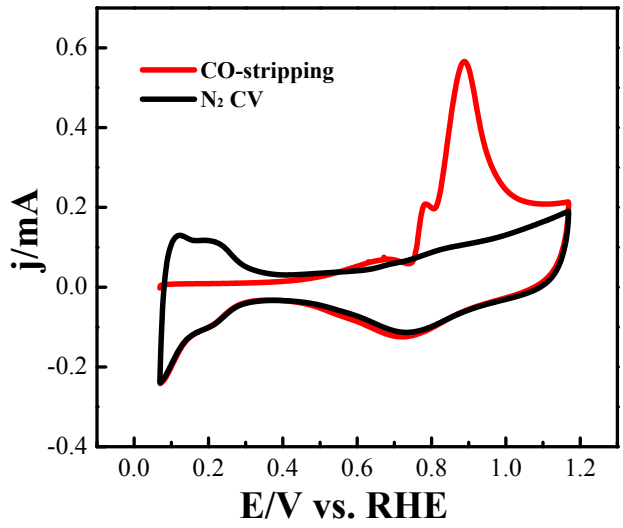

Fig. S10 CO-stripping voltammograms over commercial Pt/C in a CO-saturated 0.1 M $HClO_4$ solution at a scan rate of 50 $mV \cdot s^{-1}$.

Table S1. The atomic percentage of different elements in various catalysts.

	Pt (at.%)	Cu (at.%)	N (at.%)	O (at.%)	C (at.%)
PtCu-N	6.79	3.68	4.47	17.89	67.18
PtCu	1.04	0.7	1.23	20.7	76.33

Table S2. Summary of literature catalytic parameters of various Pt-based MOR catalyst.

Catalysts	Electrolyte	MA ($A\ mg_{Pt}^{-1}$)	SA ($mA\ cm_{Pt}^{-2}$)	Ref.
PtCu-N	0.5 M H_2SO_4 +1.0 M CH_3OH	3.11	2.73	This work
PtCu	0.5 M H_2SO_4 +1.0 M CH_3OH	1.71	2.33	This work
$Pt_{17}Pd_{16}Ru_{22}Te_{45}$ NTs	0.5 M H_2SO_4 + 1.0 M CH_3OH	1.2615	2.96	8
Pt–Mn–Cu RP	0.5 M H_2SO_4 + 2 M CH_3OH	0.65	5.85	9
Pt–Fe–Mn UCNC	0.5 M H_2SO_4 + 2 M CH_3OH	0.95	9.31	10
PtRuCu/C	0.1 M HClO4 + 1 M CH_3OH	1.35	5.22	11
200C Pt NTAs/CFC	0.5 M H_2SO_4 + 0.5 M CH_3OH	0.815	0.550	12
PtZn/MWNT-E	0.5 M H_2SO_4 + 1 M CH_3OH	<0.6	<1.1	13
PtMo nanowires	0.1 M H_2SO_4 + 1 M CH_3OH	0.984	1.6	14

Pt NP/LDG	1 M H_2SO_4 + 2 M CH_3OH	0.5962	--	15
Pt/H-TiO_2@NHPCN-800	0.5 M H_2SO_4 + 1.0 M CH_3OH	0.695	1.13	16
graphene–MWCNTs/Pt	0.5 M H_2SO_4 + 1 M CH_3OH	0.16825	--	17
Pt NWs	0.1 M $HClO_4$ + 0.1 M CH_3OH	1.312	5.84	18
$CuPt_3$ wavy nanowires	0.5 M H_2SO_4 + 0.5 M CH_3OH	0.634	2.80	19
Pt_3Co NWs/C	0.1M $HClO_4$+0.2 M CH_3OH	1.02	1.95	20
$PtCu_{2.1}$ NWs	0.1M $HClO_4$+0.2 M CH_3OH	1.56	3.31	21
PtNiCo@C–N NCs	0.5 M H_2SO_4 +1.0 M CH_3OH	1.165	1.6	22

Table S3. Summary of literature catalytic parameters of various Pt-based ORR catalysts.

Catalysts	$E_{1/2}$ V vs. RHE	MA @ 0.9V (A mg_{Pt}^{-1})	SA @0.9V (mA cm_{Pt}^{-2})	Ref.
PtCu-N	0.927	1.23	1.16	This work
PtCu	0.844	0.44	1.07	This work
Pd@$Pt_{1.8}$Ni	--	0.79	0.45	23
PtNi frame	--	0.24	0.44	24
Pt-LSSUs@PAA	0.862	--	--	25

D-$PtCo_3$	--	0.46	1	26
PtCo/C-700	0.91	0.5	0.63	27
Pt@mPt CBNs	0.9	--	0.89	28
TiNiN@Pt	0. 893	0.83	0.49	29
Pt/40Co-NC-900	0.92	<0.3	1.15	30
Pt−Rh−Ni/C	--	1.14		31
$Au_{50}Pt_{50}$	--	<0.25	0.55	32
PtNiCo@C–NCs	0.84	--	--	22
HP-Ag/Pt	0.9	0.438	0.473	33

References

1. G. Kresse, J. Furthmüller, Phys. Rev. B 1996, 54, 11169-11186.

2. G. Kresse, D. Joubert, Phys. Rev. B 1999, 59, 1758-1775.

3. J. P. Perdew, K. Burke, M. Ernzerhof, Phys. Rev. Lett. 1996, 77, 3865-3868.

4. H. J. Monkhorst, J. D. Pack, Phys. Rev. B 1976, 13, 5188-5192.

5. I. C. Man, H. Y. Su, F. Calle-Vallejo, H. A. Hansen, J. I. Martínez, N. G. Inoglu, J. Kitchin, T. F. Jaramillo, J. K. Nørskov, J. Rossmeisl, ChemCatChem. 2011, 3, 1159-1165.

6. L. Yu, X. Pan, X. Cao, P. Hu, X. Bao, J. Catal. 2011, 282, 183-190.

7. S. Kattel, P. Atanassov, B. Kiefer, J. Phys. Chem. C 2012, 116, 17378-17383.

8. S. Y. Ma, H. H. Li, B. C. Hu, X. Cheng, Q. Q. Fu and S. H. Yu, *J. Am. Chem. Soc.*, 2017, **139**, 5890-5895.

9. C. Luan, Q. X. Zhou, Y. Wang, Y. Xiao, X. Dai, X. L. Huang and X. Zhang, *Small*, 2017, **13**, 1702617-1702629.

10. C. Qin, A. Fan, X. Zhang, X. Dai, H. Sun, D. Ren, Z. Dong, Y. Wang, C. Luan, J. Y. Ye and S. G. Sun, *Nanoscale*, 2019, **11**, 9061-9075.

11. S. Xue, W. Deng, F. Yang, J. Yang, I. S. Amiinu, D. He, H. Tang and S. Mu, *ACS Catal.*, 2018, **8**, 7578-7584.

12. H. Zhang and C. Cheng, *J. Mater. Chem. A*, 2016, **4**, 15961-15967.

13. Z. Qi, C. Xiao, C. Liu, T. W. Goh, L. Zhou, R. Maligal-Ganesh, Y. Pei, X. Li, L. A. Curtiss and W. Huang, *J. Am. Chem. Soc.*, 2017, **139**, 4762-4768.

14. S. Lu, K. Eid, M. Lin, L. Wang, H. Wang and H. Gu, *J. Mater. Chem. A*, 2016, **4**, 10508-10513.

15.H. Huang, L. Ma, C. S. Tiwary, Q. Jiang, K. Yin, W. Zhou and P. M. Ajayan, *Small*, 2017, **13**. 1603013-1603021.

16.J. Zhang, X. Liu, A. Xing and J. Liu, *ACS Appl. Mater. Interfaces*, 2018, **1**, 2758-2768.

17.D. B. Gorle and M. A. Kulandainathan, *J. Mater. Chem. A*, 2017, **5**, 15273-15286.

18.L. Bu, Y. Feng, J. Yao, S. Guo, J. Guo and X. Huang, *Nano Research*, 2016, **9**, 2811-2821.

19.G. Fu, X. Yan, Z. Cui, D. Sun, L. Xu, Y. Tang, J. B. Goodenough and J. M. Lee, *Chem Sci.*,

2016, **7**, 5414-5420.

20.L. Bu, S. Guo, X. Zhang, X. Shen, D. Su, G. Lu, X. Zhu, J. Yao, J. Guo and X. Huang, *Nat. Commun.*, 2016, **7**, 11850-11860.

21.N. Zhang, L. Bu, S. Guo, J. Guo and X. Huang, *Nano Lett.*, 2016, **16**, 5037-5043.

22.Q. Wang, Q. Zhao, Y. Su, G. Zhang, G. Xu, Y. Li, B. Liu, D. Zheng and J. Zhang, *J. Mater. Chem. A*, 2016, **4**, 12296-12307.

23.X. Zhao, S. Chen, Z. Fang, J. Ding, W. Sang, Y. Wang, J. Zhao, Z. Peng and J. Zeng, *J. Am. Chem. Soc.*, 2015, **137**, 2804-2807.

24.S. Chen, Z. Niu, C. Xie, M. Gao, M. Lai, M. Li and P. Yang, *ACS Nano*, 2018, **12**, 8697-8705.

25.G.-R. Xu, B. Wang, J.-Y. Zhu, F.-Y. Liu, Y. Chen, J.-H. Zeng, J.-X. Jiang, Z.-H. Liu, Y.-W. Tang and J.-M. Lee, *ACS Catal.*, 2016, **6**, 5260-5267.

26.Q. Jia, K. Caldwell, K. Strickland, J. M. Ziegelbauer, Z. Liu, Z. Yu, D. E. Ramaker and S. Mukerjee, *ACS Catal.*, 2015, **5**, 176-186.

27.Y. Cai, P. Gao, F. Wang and H. Zhu, *Electrochimica Acta*, 2017, **245**, 924-933.

28.H. Wang, S. Yin, K. Eid, Y. Li, Y. Xu, X. Li, H. Xue and L. Wang, *ACS Sustainable Chem. Eng.* 2018, **6**, 11768-11774

29.X. Tian, J. Luo, H. Nan, H. Zou, R. Chen, T. Shu, X. Li, Y. Li, H. Song, S. Liao and R. R. Adzic, *J. Am. Chem. Soc.*, 2016, **138**, 1575-1583.

30.X. X. Wang, S. Hwang, Y. T. Pan, K. Chen, Y. He, S. Karakalos, H. Zhang, J. S. Spendelow, D. Su and G. Wu, *Nano Lett.*, 2018, **18**, 4163-4171.

31.V. Beermann, M. Gocyla, E. Willinger, S. Rudi, M. Heggen, R. E. Dunin-Borkowski, M. G. Willinger and P. Strasser, *Nano Lett.*, 2016, **16**, 1719-1725.

32.L. Zhang, S. Yu, J. Zhang and J. Gong, *Chem Sci.*, 2016, **7**, 3500-3505.

33.T. Fu, J. Fang, C. Wang and J. Zhao, *J. Mater. Chem. A*, 2016, **4**, 8803-8811.